Defect Chemistry of the Mixed Conducting Cage Compound $Ca_{12}Al_{14}O_{33}$[*]

J. Janek[†] and D.-K. Lee[‡]

Institute of Physical Chemistry, Justus-Liebig-University, Heinrich-Buff-Ring 58, D-35392 Giessen, Germany

ABSTRACT

The electrical transport properties of mayenite ($Ca_{12}Al_{14}O_{33}$ or $12\,CaO \cdot 7Al_2O_3$; mostly abbreviated as $C_{12}A_7$) can be controlled in a wide range by varying the oxygen deficiency: At high temperatures mayenite becomes either an oxygen solid electrolyte, a mixed ionic/electronic conductor or an inorganic electride with metal-like properties upon chemical reduction (removing oxygen). The underlying defect chemistry can be understood on the basis of a relatively simple model – despite the complex cage structure: A point defect model based on the assumption that the framework $[Ca_{12}Al_{14}O_{32}]^{2+}$ acts as a pseudo-donor describes well the high temperature transport properties. It accounts for the observed conductivity plateau at higher oxygen activities and also describes the experimentally observed oxygen activity dependence of the electronic conductivity with $-1/4$ slope at temperatures between 800 and $1000°$C. Doping effects in mayenite are still not well explored, and we review briefly the existing data on doping by different elements. Hydration of mayenite plays a crucial role, as Mayenite is hygroscopic, which may be a major obstacle for technical applications.

Key words : Mayenite, $Ca_{12}Al_{14}O_{33}$, Electronic conductivity, Ionic conductivity, Defect structure, $C_{12}A_7$

1. Introduction

Mayenite ($Ca_{12}Al_{14}O_{33}$, often denoted as $C_{12}A_7$ to which the quasi-binary compound $12\,CaO \cdot 7Al_2O_3$ is abbreviated) has recently become an extensively studied mixed conducting ceramic.[1] Its high ionic conductivity was first reported in 1988 by Lacerda et al.,[2] being roughly an order of magnitude lower than that of yttria-stabilized zirconia (being the most extensively employed oxygen electrolyte). Before this experimental report most studies on $C_{12}A_7$ had before dealt with its crystallographic cage structure.[3,4] The crystal lattice belongs to the cubic system of space group $I\bar{4}3d$ with a lattice parameter of 1.199.[4] Shortly after Lacerda's first report the same group also reported that polycrystalline C12A7 is hygroscopic and that the ionic conductivity of C12A7 degrades by hydration.[5] Lacerda et al. also were the first to show that C12A7 can be reduced chemically and becomes a mixed conductor thereupon.[6] Ten years later Sushko et al. excavated C12A7 and showed that it becomes an electride upon reduction by Ca metal or in hydrogen-bearing gas followed by UV-light irradiation.[7] Numerous experimental and theoretical studies have been made thereafter to reveal the transition of $C_{12}A_7$ from an ionic conductor to an electride.[8-16] Besides, the possibility of incorporation of various anions *e.g.*, halides (F^-, Cl^-),[3] oxygen radicals (O_2^-, O^-),[17,18] and hydroxide (OH^-)[19] into the C12A7 lattice forms another interesting feature of mayenite which has been studied also in some detail.

These rather specific transport properties can be attributed to the cage structure of crystalline C12A7: The framework of $Ca_{12}Al_{14}O_{33}$ is made up of a 3-dimensional network of corner-sharing AlO_4 tetrahedra together with seven-coordinated Ca ions, and six crystallographic cages of a sub-nanometer size (~0.4 nm in diameter) therein (Fig. 1). An additional oxygen ion, which is called 'free oxygen' or 'extra-framework oxygen' (as it does not reside in cage framework), occupies one of the cages to maintain charge neutrality of the crystal. The free oxygen is loosely bound to the cage with six Ca^{2+},[4] and the high ionic conductivity and the possibility of replacement of oxygen by electrons and/or another anions are easily understood.

The detailed defect structure of this interesting oxide system, however, has not been systematically explored yet, in particular with respect to doping effects. Hosono and his coworkers determined the electronic charge carrier concentration for different degrees of reduction, but a systematic study of the nonstoichiometry of C12A7 has yet not been published. The partial ionic and electronic conductivites at elevated temperature as a function of oxygen activity (from pure oxygen to low oxygen activities) have been studied by Lee and Janek.[20] And recently, Kim et al. reported on the thermoelectric properties of Mayenite for different electronic charge carrier concentrations.[21] Interestingly, the oxygen hyperstoichiometry, as caused by O_2^- or O_2^{2-} species has yet not been explored quantitatively. In the following,

[†]Corresponding author : J. Janek
E-mail : Juergen.Janek@phys.Chemie.uni-giessen.de
Tel : +49-641-99-34515   Fax : +49-641-99-34509
[‡]Current Address: Solar Cell Center, Korea Institute of Science and Technology (KIST), Seoul, 136-791, Korea; E-mail: dklee@kist.re.kr
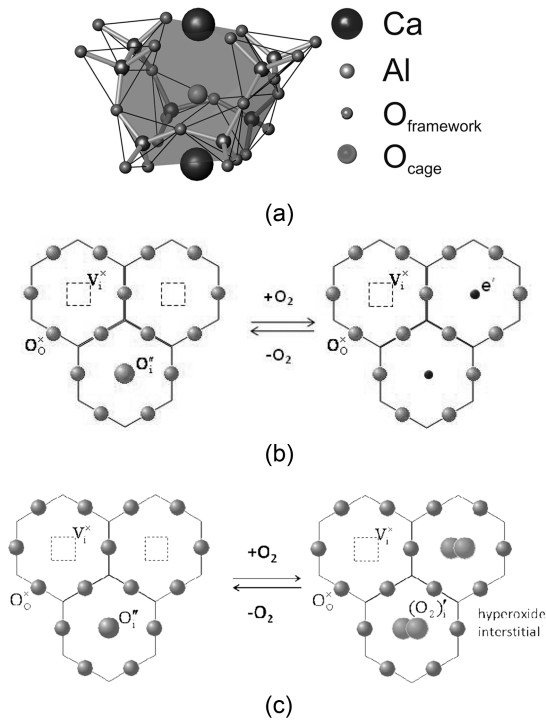
(a)

(b)

(c)

Fig. 1. (a) Illustration of $Ca_{12}Al_{14}O_{33-\delta}$ crystal lattice (reproduced by permission of the PCCP owner societies). (b) Illustration of the reduction process leading to the formation of cage electrons and (c) illustration of the incorporation of excess oxygen as hyperoxide species.

we summarize the existing understanding of C12A7 from the viewpoint of defect chemistry.

2. Defect chemistry of $Ca_{12}Al_{14}O_{33}$

West et al. demonstrated by concentration cell experiments that the total conductivity measured in laboratory air is attributed to doubly charged oxide ions.[2,22] The question arises whether this fairly high ionic conductivity originates from intrinsic defects, or has an extrinsic origin as is the case with other electrolytes, e.g. YSZ[23] or GDC.[24]

Mayenite, $C_{12}Al_{14}O_{33}$ has two types of oxide anions, one (framework oxygen) belonging to the aluminate framework formed by eightfold corner-sharing tetrahedra, $[Al_{14}O_{32}]^{22-}$ and the other (cage oxygen; free oxygen) randomly distributed within the cages of the framework. The stoichiometric mayenite crystal consists of the positively charged framework $[Ca_{12}Al_{14}O_{32}]^{2+}$ per molecular formula unit, forming six crystallographic cages. The additional oxygen ion occupies one of six chemically equivalent cages randomly. Thus, mayenite inherently has 5/6 of empty out-of-framework oxygen sites (cage sites) as structural vacancies. In stoichiometric $C_{12}A_7$, i.e., $[Ca_{12}Al_{14}O_{32}]^{2+}:(O^{2-})$ or $C_{12}A_7:O^{2-}$, however, the remaining five cages are no more equivalent to the 'free oxygen' sites because the occupation of cages by oxygen ions results in the distortion of the lattice. From the defect-chemical viewpoint it is the main question of how the cage oxygen
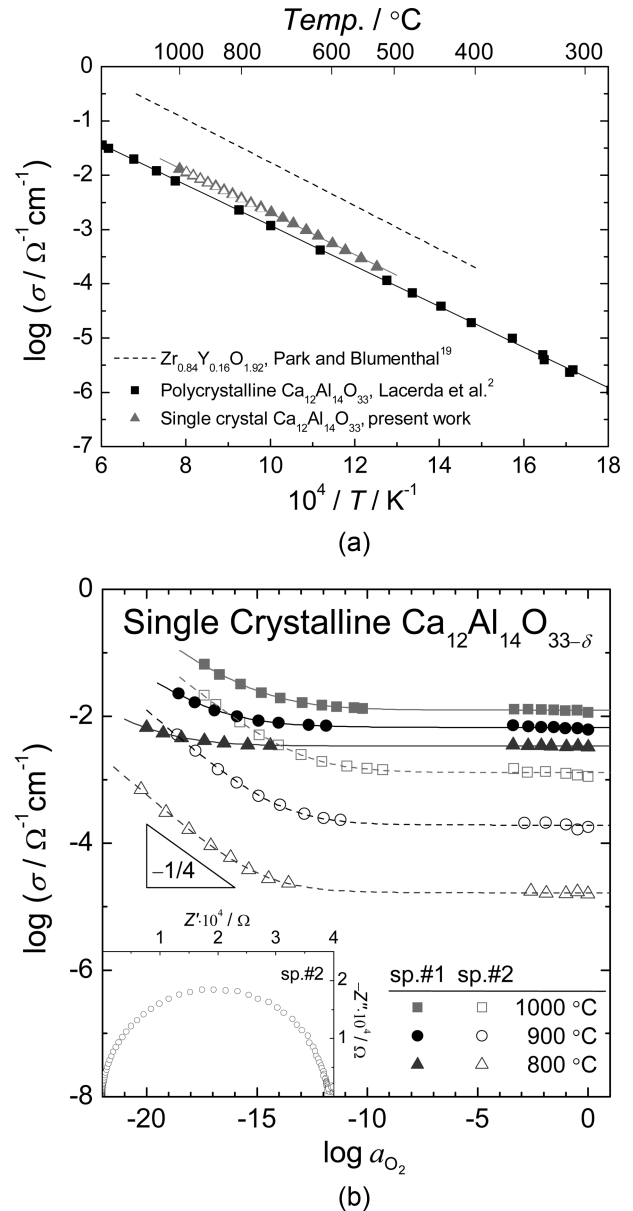

(a)

(b)

Fig. 2. Total electrical conductivity σ of single crystalline $Ca_{12}Al_{14}O_{33-\delta}$: (a) log σ in dry air vs. reciprocal temperature, (b) log σ vs. oxygen activity at different temperatures for specimen #1 (solid symbol) measured in dry condition and for specimen #2 (open symbol) in laboratory humidity after six months' annealing at 900°C. Inset in (b) shows the typical impedance response of specimen #2. The solid and dashed curves in (b) are the best-fitted to Eq. (12).

and empty cages have to be formally described in order to develop a correct defect model of mayenite.

Hosono and his group[25] described the reduction equilibrium of $C_{12}A_7$ with CO_2/CO gas mixture using building units such as O^{2-}(cage) and e^-(cage). Their straightforward treatment describes the reduction regime relatively well, but it is too simple as a general model: The charge neutrality condition, $2 \cdot x(O^{2-}) + x(e^-) = 2$ with x being mole fraction of each species, which they proposed, does not describe i) p-type
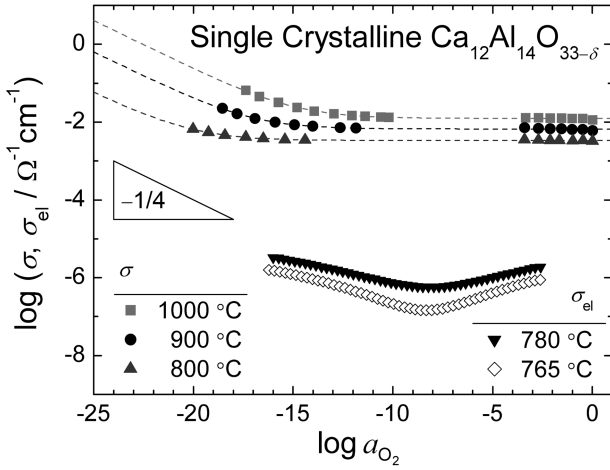
Fig. 3. Electronic partial conductivities σ_{el} *vs.* oxygen activity at different temperatures of single crystalline mayenite. Total conductivities in Fig. 2(b) are also represented for comparison purpose.

electronic conductivity (Fig. 3) ii) hyper-stoichiometry,[26-28] *i.e.*, $\delta < 0$ in Ca$_{12}$Al$_{14}$O$_{33\text{-}\delta}$(any excess oxygen would result in a negative concentration of electrons according to their charge neutrality equation); iii) the constant concentration of ionic carriers with the concomitant increase of the electron concentration as oxygen activity decreases over a wide range.

The electronic structure of C$_{12}$A$_7$, in particular, the spatial distribution of electrons introduced in place of oxygen ions upon reduction has been a subject of intense discussion. Sushko et al.[7] proposed that the extra electron in C$_{12}$A$_7$ is localized in a cage acting as a polaron or a quasi-anion, thus supporting the electride model. Medvedeva et al.[13,14] revealed by first-principle calculation of the electronic structure of [Ca$_{12}$Al$_{14}$O$_{32}$]$^{2+}$:(2e$^-$) or C$_{12}$A$_7$:2e$^-$ that the conduction electrons are highly delocalized in the cages as well as in the regions occupied with cations. Pseudo-potential plane calculations by Li et al.,[15] on the other hand, showed that the electron density is equally distributed, but being localized in the 6 cages with nonstoichiometry. In a more recent theoretical study, Sushko et al.[11] suggested that the electronic structure of C$_{12}$A$_7$:(O^{2-})$_{1\text{-}x}$(e$^-$)$_{2x}$ ($0 \leq x \leq 1$) undergoes a gradual transition from localized state to delocalized one over the cages with increasing electron concentration x, which was also experimentally verified by Matsuishi et al.[12] who demonstrated a change of conduction mechanism of electron from hopping to metallic one with increasing x. The most recent structural study using synchrotron X-ray diffraction by Palacios et al.[16] showed electron density localized into the center of the cages in C$_{12}$A$_7$:(O^{2-})$_{0.55}$(e$^-$)$_{0.9}$.

2.1. Partial electrical conductivities

One may regard the framework of C$_{12}$A$_7$, *i.e.*, [Ca$_{12}$Al$_{14}$O$_{32}$]$^{2+}$, acting as a doubly charged pseudo-donor, D$_{FW}^{\bullet\bullet}$, of which concentration is fixed by the molecular density ($\beta \equiv N_A/V_m = 1.16 \times 10^{21}$ cm^{-3} where N_A, V_m are Avogadro's number, molar volume of C$_{12}$A$_7$), and six cages as neutral

interstitial sites, I$_i^x$ (regular structure element). The extra-framework oxygen (cage oxygen; free oxygen) may then be treated as doubly ionized interstitial oxygen, O$_i''$ (irregular structure element) in terms of Kroeger-Vink notation. Since there are five additional cages, I$_i^x$, for stoichiometric mayenite, C$_{12}$A$_7$:(O^{2-}), we can assume that a thermal equilibrium (anti-Frenkel type disorder) may give rise to a fraction of framework oxygen, O$_O^x$, residing at the interstitial sites leaving the corresponding number of lattice oxygen vacancies V$_O^{\bullet\bullet}$ in the framework. Equilibrium for electron (e$'$)-hole (h$^\bullet$) pair formation is also assumed. Accepting the theoretical results for a gradual change of the electron localization,[11,12] it is reasonable to represent electrons as e$_i'$ as long as the degree of reduction of is much less than the metal/metal oxide equilibrium in which the transition is reported to be complete.[12] Taking into account all relevant structure elements, the charge neutrality condition is then given as

$$2[D_{FW}^{\bullet\bullet}] + 2[V_O^{\bullet\bullet}] + p = 2[O_i''] + n \quad \text{or}$$

$$2\beta + 2[V_O^{\bullet\bullet}] + p = 2[O_i''] + n \tag{1}$$

along with external (reduction) and internal equilibria as

$$O_i'' + I_i^x = 2e_i' + \frac{1}{2}O_2(g); \quad K_R = \frac{n^2}{[O_i'']} \cdot a_{O_2}^{1/2} \tag{2}$$

$$O_O^x + I_i^x = V_O^{\bullet\bullet} + O_i'', \quad K_{AF} = [V_O^{\bullet\bullet}] \cdot [O_i''] \tag{3}$$

$$null = e' + h^\bullet; \quad K_i = n \cdot p \tag{4}$$

where [D] stands for the concentration of defect species D (= D$_{FW}^{\bullet\bullet}$, O$_i''$, V$_O^{\bullet\bullet}$), and n, p for the concentration of electrons and holes, in cm^{-3}, respectively. K_j denotes the equilibrium constant for the associated reaction j (j = R, AF, i). The non-stoichiometry, δ, the deviation from the (electronic) stoichiometic composition ($\delta \equiv 0$), is defined as

$$\beta\delta = [V_O^{\bullet\bullet}] - ([O_i''] - [D_{FW}^{\bullet\bullet}]) = \frac{1}{2}(n - p) \tag{5}$$

The electronic defect concentration can be characterized with the oxygen nonstoichiometry δ as Ca$_{12}$Al$_{14}$O$_{33\text{-}\delta}$. Four majority disorder types can be distinguished from Eq. (1) to get the solution to Eqs. (1)~(4) as shown in Fig. 4: As the oxygen activity increases, the disorder type shifts from (V$_O^{\bullet\bullet}$, e$'$) to (e$'$, D$_{FW}^{\bullet\bullet}$) to (D$_{FW}^{\bullet\bullet}$, O$_i''$) to (O$_i''$, h$^\bullet$), in turn.

In the near stoichiometric regime ($n \approx p$), the positively charged pseudo-donor, D$_{FW}^{\bullet\bullet}$, is compensated by interstitial oxygen, O$_i''$, that is, Eq. (1) can be simplified as

$$[D_{FW}^{\bullet\bullet}] \approx [O_i''] \tag{6}$$

Combining Eqs. (2), (4) and (6), the concentration of electronic charge carriers, n and p, are calculated respectively as

$$n \approx \sqrt{K_i}\left(\frac{a_{O_2}}{a_{O_2}^\circ}\right)^{-1/4}, \quad p \approx \sqrt{K_i}\left(\frac{a_{O_2}}{a_{O_2}^\circ}\right)^{+1/4} \tag{7}$$

Here $a_{O_2}^\circ$ is the oxygen activity corresponding to the stoichiometric composition ($\delta \equiv 0$) where $n = p = K_i^{1/2}$. Similarly,

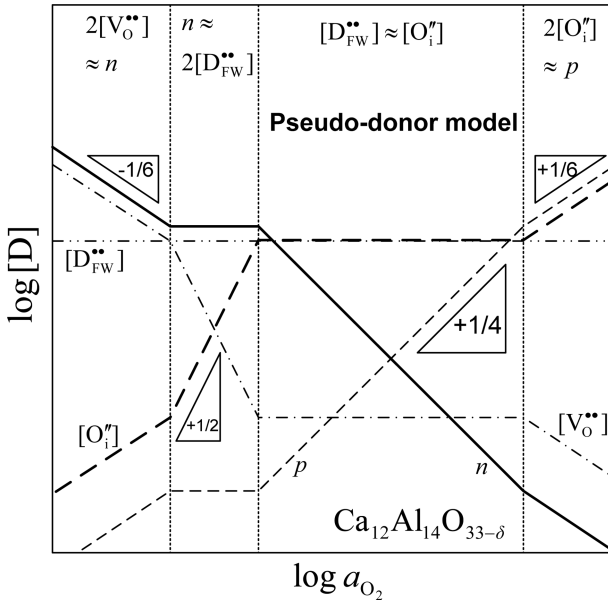**Fig. 4.** Kroeger-Vink diagram of $Ca_{12}Al_{14}O_{33-\delta}$. The vertical dashed lines are the boarders between different majority disorder regimes and the numbers inside triangles denote the oxygen exponents m such that $[D] \propto a_{O_2}^m$.

Fig. 5. Mobility of oxygen interstitial for single crystalline $Ca_{12}Al_{14}O_{33-\delta}$.

by solving Eqs. (2)~(4) with simplified charge neutrality constraints, $2[V_O^{\bullet\bullet}] \approx n$, $n \approx 2[D_{FW}^{\bullet\bullet}]$, $[D_{FW}^{\bullet\bullet}] \approx [O_i'']$, $2[O_i''] \approx p$, in tandem, one can represent the defect diagram of mayenite as illustrated in Fig. 4.

The migration of oxygen may take place with the aid of interstitials O_i'' and/or vacancies $V_O^{\bullet\bullet}$: i) an extra-framework oxygen O_i'' displaces a neighboring framework oxygen $O_O^\times$ into an another empty cage site $I_i^\times$ and itself taking the place of the displaced lattice ion (interstitialcy mechanism); ii) an interstitial oxygen O_i'' moves between adjacent interstitial sites through the opening on the cage wall (interstitial mechanism); iii) a lattice oxygen $O_O^\times$ exchanges its position with a vacancy $V_O^{\bullet\bullet}$ (vacancy mechanism). Theoretical calculations shows that the interstitialcy mechanism is energetically most favored in mayenite crystal,[29] which is in line with a neutron diffraction study.[26] An ^{18}O exchange experiment followed by Raman spectroscopy[30] indicates that the local fraction of ^{18}O is equal between the framework and extra-framework sites, thus implying that the exchange of the oxygen ion in the framework, $O_O^\times$, can be easily achieved with the extra-framework oxygen, O_i'', consequently supporting the interstitialcy mechanism.

When the oxygen transport takes place *via* interstitialcy mechanism, the oxygen ion conductivity, σ_O, can be expressed as

$$\sigma_O = [\beta \cdot x(O_i'')] \cdot 2e \cdot u(O_i'') \cdot \frac{x(I_i^\times)}{6} \qquad (8)$$

where $x(D)$, e, and $u(O_i'')$ denote mole fraction of defect species (that is, $\beta \cdot x(O_i'')$ represents the concentration of mobile

oxygen interstitial in cm^{-3}), elementary charge, and electrochemical mobility of oxygen interstitial, respectively. It is noted that $x(I_i^\times)/6$ reflects the probability of successful jumps of a displaced oxygen, $O_O^\times$, into a vacant interstitial site, $I_i^\times$. It is readily recognized that both $x(O_i'')$ and $x(I_i^\times)$ are constant as 1 and 5, respectively, due to Eq. (6) and site conservation constraint, $x(O_i'') + x(I_i^\times) = 6$, in the near stoichiometry regime. The observed total conductivity that remains unchanged in the oxygen activity range of $-15 < \log a_{O_2} \leq 0$ in Fig. 2(b) is compatible with the present model that accounts for the ionic charge carrier concentration independent of oxygen activity. It is emphasized here that the high ionic conductivity in $Ca_{12}Al_{14}O_{33}$ is a consequence of intrinsic crystal structure without additional doping.

The mobility of the oxygen interstitial as a function of reciprocal temperature from Eq. (8) as determined by Lee and Janek[20] is shown in Fig. 5. The calculated mobility, which is represented by linear regression as

$$u(O_i'')/cm^2V^{-1}s^{-1} = \frac{2.36 \times 10^{1.00 \pm 0.02}}{T}$$

$$\cdot \exp\left[-\frac{(0.845 \pm 0.003)eV}{kT}\right] \qquad (9)$$

takes a value of $2.4 \times 10^{-6} < u(O_i'')/cm^2V^{-1}s^{-1} < 8.3 \times 10^{-6}$ in the temperature range of $1073 \leq T / K \leq 1273$.

As the oxygen activity decreases, on the other hand, the reduction of $C_{12}A_7$ may proceed in such a way that the cage oxygen, O_i'', is replaced by electron as described by Eq. (2). The reduction equilibrium can be schematically illustrated in an electron energy diagram as shown in Fig. 6, where solid and dotted bars represent the occupied electronic states of the oxygen interstitial (cage oxygen; free oxygen) and the vacant interstitial site (cage) that are spatially isolated, and the arrow the electron with two spin states. The electron mobility of $C_{12}A_7$ were reported as $u_n/cm^2V^{-1}s^{-1} =$
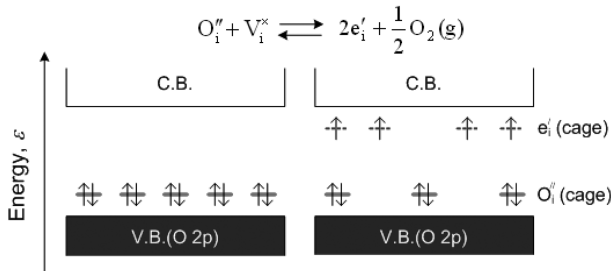
Fig. 6. Schematic of the change in electronic structure of $Ca_{12}Al_{14}O_{33-\delta}$ by reduction. The occupied electronic states of oxygen interstitials and vacant interstitial sites are denoted by solid and dotted bars, and electrons by arrows.

0.34 (calculated from Ref. 25) or 0.1 for hopping electrons[31] and $u_n/cm^2V^{-1}s^{-1}=4$ for the electron in conduction band,[31] respectively, at room temperature. By comparing the reported values for the mobility of electron with that for the oxygen interstitial evaluated above, it can be deduced that the observed conductivity variation in the reducing condition, $\sigma \propto a_{O_2}^{-1/4}$ in Fig. 2(b), also belongs to the regime of $[D_{FW}^{\bullet\bullet}] \approx [O_i'']$ in the defect diagram (Fig. 4) with predominant ionic defect concentrations but with overwhelming electronic carrier mobilities.

The present defect model further anticipates that in the far reducing atmosphere the electron concentration will be saturated to a value of $2\beta=2.32\times10^{21}$ cm^{-3} due to the electronic compensation, $i.e.$, $n \approx 2[D_{FW}^{\bullet\bullet}]$. By reduction with Ca or Ti metals,[9,31] Hosono et al. have achieved extremely low oxygen activities corresponding to the equilibrium between metal and metal oxide and came close to this limit. Matsuishi et al. reported that $C_{12}A_7$ reduced by Ca at 700°C for 240 h, thereby showing temperature-independent conductivity, contained 2×10^{21} cm^{-3} of electrons, and claimed that this value agreed well with the theoretical maximum of 2.33 $\times10^{21}$ cm^{-3}.[9] However, the electron concentration in the crystal reduced by Ti at 900°C for 24 h, of which conductivity is quite similar to the former in magnitude as well as in temperature dependence, was found to be 0.97×10^{21} cm^{-3}.[31] Due to such an uncertainty it seems not really clear whether there is an achievable limit of the electron concentration in mayenite. We note that the validity of the pseudo-donor model can be more unambiguously demonstrated by identifying the saturation in the electron concentration with decreasing a_{O_2}, and that even higher electronic conductivity may be achieved if $C_{12}A_7$ is made to reach the defect regime of $(V_O^{\bullet\bullet}, e')$.

2.2. Ionic transference number

Summing up Eqs. (6) and (7), the conductivity isotherm as the sum of n-type conductivity σ_n and constant ionic conductivity σ_o in the experimental condition of the present study, can be represented as

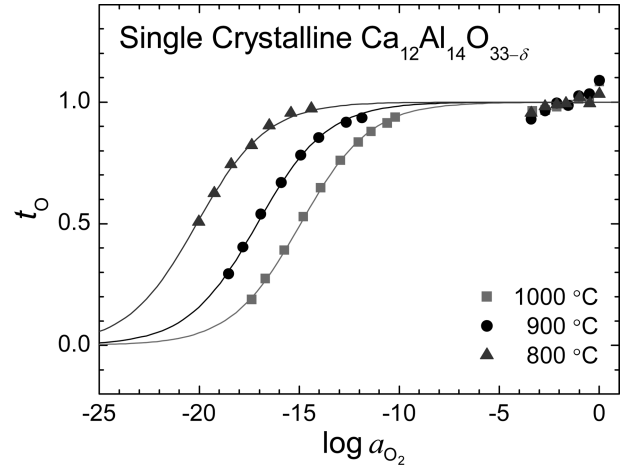$$\sigma = \sigma_n^\circ \cdot a_{O_2}^{-1/4} + \sigma_O \qquad (10)$$

Fig. 7. Ionic transference number t_O $vs.$ log a_{O_2} for single crystalline $Ca_{12}Al_{14}O_{33-\delta}$ (specimen #1) at different temperatures. The solid lines are the calculated via Eq. (11).

based on the assumption that the mobilities of electronic and ionic carriers are independent of oxygen activity. Here, σ_n° denotes the electronic partial conductivity at $a_{O_2}=1$. The measured total conductivity was fitted by Eq. (10) as depicted by solid and dashed curves in Fig. 2(b), see Lee and Janek[20] for details.

The ionic transference number t_O $(\equiv \sigma_O / \sigma)$ by using the numerical values for σ_O and σ_n° results as

$$t_O = \frac{\sigma_O}{\sigma_O + \sigma_n^\circ a_{O_2}^{-1/4}} \qquad (11)$$

Fig. 7 shows t_O as a function of oxygen activity where the solid curves are calculated via Eq. (11). The ionic transference number t_O of $C_{12}A_7$ remains almost unity in the oxygen activity range of log $a_{O_2} > -8$ (ion conducting), and then decreases with decreasing a_{O_2} finally to the value close to 0 at around log $a_{O_2} = -20$ (electron conducting). The isothermal variation of t_O from 1 to 0, bridging two remarkable properties of $C_{12}A_7$ as an electrolyte and an electride, clearly demonstrates the chemical route for its transition.

2.3. Hydration mechanism

Very early Lacerda reported that polycrystalline C12A7 is hygroscopic and that the ionic conductivity of C12A7 degrades by hydration.[5] Details on the hydration of mayenite have yet only been reported by Lee and Janek[20] and by Strandbakke et al..[32] Lee and Janek studied the temporal evolution of the ionic conductivity upon hydration and found contradictory results, suggesting that the detailed mechanism of hydration in mayenite is far from simple: They found i) a short-term increase of conductivity (by about 40%,) upon hydration using a water-saturated gas mixture (p_{H_2O} / 10^5 Pa $= 2.1\times10^{-2}$) in a fixed oxygen partial pressure; ii) a long-term degradation at 900°C in a laboratory humidity.

Irvine and West[5] suggested that water uptake leads to the formation of immobile hydroxides and hence reduces the
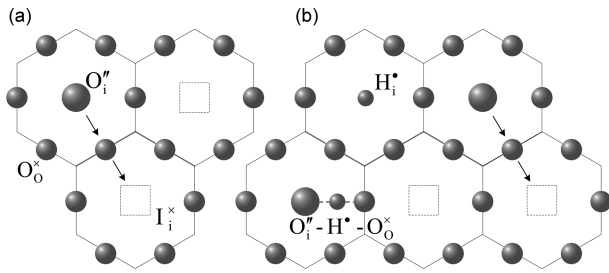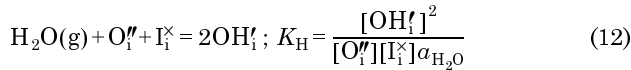
Fig. 8. Schematic illustration of the oxygen transport in $Ca_{12}Al_{14}O_{33-\delta}$; (a) in dry condition, and (b) during hydration. Note that metal ions are not shown.

ionic conductivity. The proposed hydration reaction may be rewritten in terms of Kroeger-Vink notation as
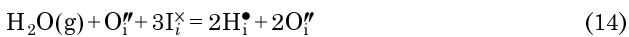
$$H_2O(g) + O_i'' + I_i^\times = 2OH_i' \; ; \; K_H = \frac{[OH_i']^2}{[O_i''][I_i^\times]a_{H_2O}} \quad (12)$$

It has been reported that the $C_{12}A_7$ uptakes up to 1.12 wt% H_2O after annealing in air of normal humidity at 960°C,[3] resulting in the composition close to $C_{12}A_7$:$(OH^-)_2$, *i.e.*, $[Ca_{12}Al_{14}O_{32}]\,(OH^-)_2$ (note that the incorporation of 1.3 wt% of H_2O leads to the exact stoichiometric composition). By combined analysis of IR spectroscopy with thermodynamics, Hayashi et al.[33] demonstrated that hydration proceeds with the surface reaction *via* Eq. (12) followed by the chemical diffusion of O^{2-} and OH^- ions, and the rate determining process of the latter is the inward bulk diffusion of OH^-. According to their kinetic analysis, the chemical diffusion coefficient of the H_2O molecule is smaller by 2 to 3 orders of magnitude than the self diffusion coefficient of oxygen ion, taking the value of $\tilde{D}_{H_2O}/cm^2 s^{-1} = 5.15 \times 10^{-10}$ at 900°C. This leads for samples with dimensions in the mm range to conductivity changes in the time range of some months.

The enhanced conductivity by 40% upon an abrupt change of atmosphere to a water-saturated one, as described by Lee and Janek, cannot be explained by Eq. (12) only. They rather suggest that the increased concentration of OH_i', which is determined by the equilibrium of the reaction Eq. (12), $[OH_i'] \propto a_{H_2O}^{1/2}$, may shift the equilibrium of the following reaction to the left.

$$2H_i^\bullet + 2O_i'' = 2OH_i' + 2I_i^\times \quad (13)$$

which, in combination with Eq. (12), leads to

$$H_2O(g) + O_i'' + 3I_i^\times = 2H_i^\bullet + 2O_i'' \quad (14)$$

Eq. (14) suggests that an incorporation of water into $C_{12}A_7$ induces the increase in the concentration of the mobile oxygen interstitial O_i'' as well as proton $H_i^\bullet$ at the very initial stage of hydration. The transference number of the latter, however, was found to be negligibly small.[34] Thus, about 40% of enhancement in electrical conductivity may be attributed to the increase of $[O_i'']$ near the surface region only in the transient state of hydration.

This scenario may be schematically represented as shown in Fig. 8(b). The interstitialcy mechanism in dry condition is also illustrated in Fig. 8(a) for comparison. The metal ions are not shown for simplicity's sake.

3. Summary and Conclusion

The electrical transport properties and their dependence on the oxygen content (*i.e.* the degree of reduction) of $C_{12}A_7$ can be well described within the framework of point defect thermodynamics. From the defect chemical point of view $C_{12}A_7$ is an interesting example for a material with a structurally fixed number of mobile ionic charge carriers. Thus, it might be considered as a structurally disordered material, like e.g. the silver superionic conductors, but a different model appears to be more appropriate: Neglecting hydration effects, the ionic and electronic disorder can be described as follows: The framework $[Ca_{12}Al_{14}O_{32}]^{2+}$ acts as a doubly charged pseudo-donor and is electrically compensated by a doubly ionized interstitial oxygen occupying one of six cages $(I_i^\times)$ such that $[D_{FW}^{\bullet\bullet}] \approx [O_i'']$, which results in the electronic concentration varying as $n \propto a_{O_2}^{-1/4}$, $p \propto a_{O_2}^{+1/4}$. Thus, $C_{12}A_7$ shows the same oxygen activity dependence of its partial conductivities as doped zirconia or ceria. The ionic transference number of $C_{12}A_7$ decreases from 1 to 0 with decreasing oxygen activity, and its oxygen activity dependence can be well understood by this simple defect model. There is still the need for a quantitative study of the exact oxygen content –*i.e.* the nonstoichiometry is still an open question.

Hydration modifies the transport properties significantly – as is expected for a compound being composed of two highly basic oxides CaO and Al_2O_3. The decrease of conductivity by about two orders of magnitude as well as the increase of its activation energy by 1.79 eV for the fully hydrated $C_{12}A_7$ compared to dry one is attributed to the formation of immobile hydroxide. First quantitative results on the hydration behavior have been reported by Strandbakke et al.[32] Also, recently Kim et al.[21] have investigated the thermoelectric transport properties of mayenite which are fully in accord with the defect model presented here.

A different description of the defect chemistry of mayenite has been proposed by Strandbakke and Norby[32] in their paper on the hydration of mayenite. They use fractional defects in order to account for the structural disorder of mayenite. Their results on the total conductivity of hydrated mayenite is in full agreement with the results by Lee and Janek.

Acknowledgments

REFERENCES

1. K. L. Scrivener, "Historical and Present Day Applications of Calcium Aluminate Cements," pp. 3-23 in *Calcium Alu-*

minate Cements 2001, ed. R. J. Mangabhai and F. P. Glasser, IOM communications Ltd., London, 2001.

2. M. Lacerda, J. T. S. Irvine, F. P. Glasser, and A. R. West, "High Oxide Ion Conductivity in $Ca_{12}Al_{14}O_{33}$," *Nature*, **332** 525-26 (1988).

3. J. Jeevaratnam, F. P. Glasser, and L. S. D. Glasser, "Anion Substitution and Structure of $12CaO \cdot 7Al_2O_3$," *J. Am. Ceram. Soc.*, **47** 105-6 (1964).

4. H. B. Bartl and T. Scheller, *Neues Jahrb. Mineral., Monatsh.*, **35** 547-52 (1970).

5. J. T. S. Irvine and A. R. West, *J. Appl. Electrochem.*, **19** 410-12 (1989).

6. M. Lacerda, A. R. West, and J. T. S. Irvine, "Electrical Properties of $Ca_{12}Al_{14}O_{33}$: Effect of Hydrogen Reduction," *Solid State Ionics*, **59** 257-62 (1993).

7. P. V. Sushko, A. L. Shluger, K. Hayashi. M. Hirano, and H. Hosono, "Electron Localization and a Confined Electron Gas in Nanoporous Inorganic Electrides," *Phys. Rev. Lett.*, **91** 126401 (2003).

8. K. Hayashi, S. Matsuishi, T. Kamiya, M. Hirano, and H. Hosono, "Light-Induced Conversion of an Insulating Refractory Oxide into a Persistent Electronic Conductor," *Nature*, **419** 462-65 (2002).

9. S. Matsuishi, Y. Toda, M. Miyakawa, K. Hayashi, T. Kamiya, M. Hirano, I. Tanaka, and H. Hosono, "High-Density Electron Anions in a Nanoporous Single Crystal: $[Ca_{24}Al_{28}O_{64}]^{4+}(4e-)$," *Science*, **301** 626-29 (2003).

10. P. V. Sushko, A. L. Shluger, K. Hayashi, M. Hirano, and H. Hosono, "Role of Hydrogen Atoms in the Photoinduced Formation of Stable Electron Centers in H-doped $12CaO \cdot 7Al_2O_3$," *Phys. Rev. B*, **73** 045120 (2006).

11. P. V. Sushko, A. L. Shluger, M. Hirano, and H. Hosono, "From Insulator to Electride: A Theoretical Model of Nanoporous Oxide $12CaO \cdot 7Al_2O_3$," *J. Am. Chem. Soc.*, **129** 942-51 (2007).

12. S. Matsuishi, S. W. Kim, T. Kamiya, M. Hirano, and H. Hosono, "Localized and Delocalized Electrons in Room-Temperature Stable Electride $[Ca_{24}Al_{28}O_{64}]^{4+}(O2-)_{2-x}(e-)_{2x}$: Analysis of Optical Reflectance Spectra," *J. Phys. Chem. C*, **112** 4753-60 (2008)

13. J. E. Medvedeva, A. J. Freeman, M. I. Bertoni, and T. O. Mason, "Electronic Structure and Light-Induced Conductivity of a Transparent Refractory Oxide," *Phys. Rev. Lett.*, **93** 016408 (2004).

14. J. E. Medvedeva and A. J. Freeman, "Hopping versus Bulk Conductivity in Transparent Oxides: $12CaO \cdot 7Al_2O_3$," *Appl. Phys. Lett.*, **85** 955-57 (2004).

15. Z. Li, J. Yang, J. G. Hou, and Q. Zhu, "Is Mayenite without Clathrated Oxygen an Inorganic Electride?," *Angew, Chem. Int. Ed.*, **43** 6479-82 (2004).

16. L. Palacios, A. Cabeza, S. Bruque, S. Garcia-Granda, and M. A. G. Aranda, "Structure and Electrons in Mayenite Electrides," *Inorg. Chem.*, **47** 2661-67 (2008).

17. H. Hosono and Y. Abe, "Occurrence of Superoxide Radical Ion in Crystalline Calcium Aluminate $12CaO \cdot 7Al_2O_3$ Prepared via Solid-State Reactions," *Inorg, Chem.*, **26** 1192-95 (1987).

18. K. Hayashi, M. Hirano, S. Matsuishi and H. Hosono, "Microporous Crystal $12CaO \cdot 7Al_2O_3$ Encaging Abundant O- Radicals," *J. Am. Chem. Soc.*, **124** 738-39 (2002).

19. J. A. Imlach, L. S. D. Glasser, and P. F. Glasser, "Excess Oxygen and the Stability of $12CaO \cdot 7Al_2O_3$," *Cement Conc. Res.*, **1** 57-61 (1971).

20. D.-K. Lee, L. Kogel, S. G. Ebbinghaus, I. Valov, H.-D. Wiemhoefer, M. Lerch, and J. Janek, "Defect Chemistry of the Cage Compound, $Ca_{12}Al_{14}O_{33-\delta}$ - Understanding the Route from a Solid Electrolyte to a Semiconductor and Electride," *Phys. Chem. Chem. Phys.*, **11**, 3105-14 (2009).

21. S. W. Kim, R. Tarumi, H. Iwasaki, H. Ohta, M. Hirano, and H. Hosono, "Thermal Conductivity and Seebeck Coefficient of $12CaO \cdot 7Al_2O_3$ Electride with a Cage Structure," *Phys. Rev. B*, **80** 075201 (2009).

22. J. T. S. Irvine, M. Lacerda, and A. R. West, "Oxide Ion Conductivity in $Ca_{12}Al_{14}O_{33}$," *Mat. Res. Bull.*, **23** 1033-38 (1988).

23. J.-H. Park and R. N. Blumenthal, "Electronic Transport in 8 Mole Percent Y_2O_3-ZrO_2," *J. Electrochem. Soc.*, **136** 2867-76 (1989).

24. M. Mogensen, T. Lindegaard, U. R. Hansen, and G.. Mogensen, "Physical Properties of Mixed Conductor Solid Oxide Fuel Cell Anodes of Doped CeO_2," *J. Electrochem. Soc.*, **141** 2122-28 (1994).

25. S.-W. Kim, K. Hayashi, M. Hirano, and H. Hosono, "Electron Carrier Generation in a Refractory Oxide $12CaO \cdot 7Al_2O_3$ by Heating in Reducing Atmosphere: Conversion from an Insulator to a Persistent Conductor," *J. Am. Ceram. Soc.*, **89** 3294-98 (2006).

26. H. Boysen, M. Lerch, A. Stys, and A. Senyshyn, "Structure and Oxygen Mobility in Mayenite ($Ca_{12}Al_{14}O_{33}$): A High-Temperature Neutron Powder Diffraction Study," *Acta Cryst.*, **B63** 675-82 (2007).

27. K. Hayashi, S. Matsuishi, M. Hirano, and H. Hosono, "Formation of Oxygen Radicals in $12CaO \cdot 7Al_2O_3$: Instability of Extraframework Oxide Ions and Uptake of Oxygen Gas," *J. Phys. Chem. B*, **108** 8920-25 (2004).

28. O. Trofymluk, Y. Toda, H. Hosono, and A. Navrotsky, "Energetics of Formation and Oxidation of Microporous Calcium Aluminates: A New Class of Electrides and Ionic Conductors," *Chem. Mater.*, **17** 5574-79 (2005).

29. P. V. Sushko, A. L. Shluger, K. Hayashi, M. Hirano, and H. Hosono, "Mechanisms of Oxygen Ion Diffusion in a Nanoporous Complex Oxide $12CaO \cdot 7Al_2O_3$," *Phys. Rev. B*, **73** 014101 (2006).

30. K. Kajihara, S. Matsuishi, K. Hayashi, M. Hirano, and H. Hosono, "Vibrational Dynamics and Oxygen Diffusion in a Nanoporous Oxide Ion Conductor $12CaO \cdot 7Al_2O_3$ Studied by ^{18}O Labeling and Micro-Raman Spectroscopy," *J. Phys. Chem. C*, **111** 14855-61 (2007).

31. S. W. Kim, S. Matsuishi, T. Nomura, Y. Kubota, M. Tanaka, K. Hayashi, T. Kamiya, M. Hirano, and H. Hosono, "Metallic State in a Lime–Alumina Compound with Nanoporous Structure," *Nano Lett.*, **7** 1138-43 (2007).

32. R. Strandbakke, C. Kongshaug, R. Haugsrud, and T. Norby, "High-Temperature Hydration and Conductivity of Mayenite, $Ca_{12}Al_{14}O_{33}$," *J. Phys. Chem. C*, **113** 8938-44 (2009).

33. K. Hayashi, M. Hirano, and H. Hosono, "Thermodynamics and Kinetics of Hydroxide Ion Formation in $12CaO \cdot 7Al_2O_3$," *J. Phys. Chem. B*, **109** 11900-906 (2005).

34. K. Hayashi, P. V. Sushko, A. L. Shluger, M. Hirano, and H. Hosono, "Hydride Ion as a Two-Electron Donor in a Nanoporous Crystalline Semiconductor $12CaO \cdot 7Al_2O_3$," *J. Phys. Chem. B*, **109** 23836-42 (2005).